

# Standardized measurement of coronary inflammation using cardiovascular computed tomography: integration in clinical care as a prognostic medical device

Evangelos K. Oikonomou <sup>1,2†</sup>, Alexios S. Antonopoulos<sup>1†</sup>, David Schottlander <sup>3</sup>,  
Mohammad Marwan<sup>4</sup>, Chris Mathers <sup>3</sup>, Pete Tomlins<sup>3</sup>, Muhammad Siddique<sup>3</sup>,  
Laura V. Klüner <sup>1</sup>, Cheerag Shirodaria <sup>3</sup>, Michail C. Mavrogiannis <sup>1</sup>,  
Sheena Thomas <sup>5</sup>, Agostina Fava<sup>6</sup>, John Deanfield<sup>7</sup>, Keith M. Channon <sup>1,8,9</sup>,  
Stefan Neubauer <sup>1,8,9</sup>, Milind Y. Desai <sup>6</sup>, Stephan Achenbach<sup>4</sup>, and  
Charalambos Antoniades <sup>1,5,8,9\*</sup>

<sup>1</sup>Division of Cardiovascular Medicine, Radcliffe Department of Medicine, University of Oxford, John Radcliffe Hospital, Headley Way, Oxford OX39DU, Oxford UK; <sup>2</sup>Section of Cardiovascular Medicine, Department of Internal Medicine, Yale School of Medicine, 333 Cedar St, New Haven, CT 06510, USA; <sup>3</sup>Caristo Diagnostics, 1st Floor, New Barclay House, 234 Botley Rd, OX2 0HP, Oxford, UK; <sup>4</sup>Department of Cardiology, Friedrich-Alexander-Universität Erlangen-Nürnberg, Maximilianspl 2, 91054 Erlangen, Germany; <sup>5</sup>Acute Vascular Imaging Centre, Radcliffe Department of Medicine, University of Oxford, John Radcliffe Hospital, Headley Way, Oxford OX39DU, Oxford UK; <sup>6</sup>Department of Cardiovascular Medicine, Cleveland Clinic, 9500 Euclid Avenue, Cleveland, OH44195, USA; <sup>7</sup>Institute of Cardiovascular Science, Faculty of Population Health Sciences, University College London, Gower Street, London WC1E 6BT; <sup>8</sup>British Heart Foundation Centre of Research Excellence, John Radcliffe Hospital, Headley Way, Oxford OX39DU, Oxford UK; and <sup>9</sup>National Institute of Health Research (NIHR), Oxford Biomedical Research Centre, Oxford University Hospitals NHS Foundation Trust, John Radcliffe Hospital, Headley Way, Oxford OX39DU, Oxford UK

Received 7 June 2021; editorial decision 23 August 2021; accepted 27 August 2021; online publish-ahead-of-print 27 August 2021

## Aims

Coronary computed tomography angiography (CCTA) is a first-line modality in the investigation of suspected coronary artery disease (CAD). Mapping of perivascular fat attenuation index (FAI) on routine CCTA enables the non-invasive detection of coronary artery inflammation by quantifying spatial changes in perivascular fat composition. We now report the performance of a new medical device, CaRi-Heart<sup>®</sup>, which integrates standardized FAI mapping together with clinical risk factors and plaque metrics to provide individualized cardiovascular risk prediction.

## Methods and results

The study included 3912 consecutive patients undergoing CCTA as part of clinical care in the USA ( $n=2040$ ) and Europe ( $n=1872$ ). These cohorts were used to generate age-specific nomograms and percentile curves as reference maps for the standardized interpretation of FAI. The first output of CaRi-Heart<sup>®</sup> is the FAI-Score of each coronary artery, which provides a measure of coronary inflammation adjusted for technical, biological, and anatomical characteristics. FAI-Score is then incorporated into a risk prediction algorithm together with clinical risk factors and CCTA-derived coronary plaque metrics to generate the CaRi-Heart<sup>®</sup> Risk that predicts the likelihood of a fatal cardiac event at 8 years. CaRi-Heart<sup>®</sup> Risk was trained in the US population and its performance was validated externally in the European population. It improved risk discrimination over a clinical risk factor-based model [ $\Delta$ (C-statistic) of 0.085,  $P=0.01$  in the US Cohort and 0.149,  $P<0.001$  in the European cohort] and had a consistent net clinical benefit on decision curve analysis above a baseline traditional risk factor-based model across the spectrum of cardiac risk.

## Conclusion

Mapping of perivascular FAI on CCTA enables the non-invasive detection of coronary artery inflammation by quantifying spatial changes in perivascular fat composition. We now report the performance of a new medical device, CaRi-Heart<sup>®</sup>, which allows standardized measurement of coronary inflammation by calculating the FAI-Score of

\* Corresponding author. Tel: +44 1865 228340; fax: +44 1865 740352, E-mail: antoniad@well.ox.ac.uk

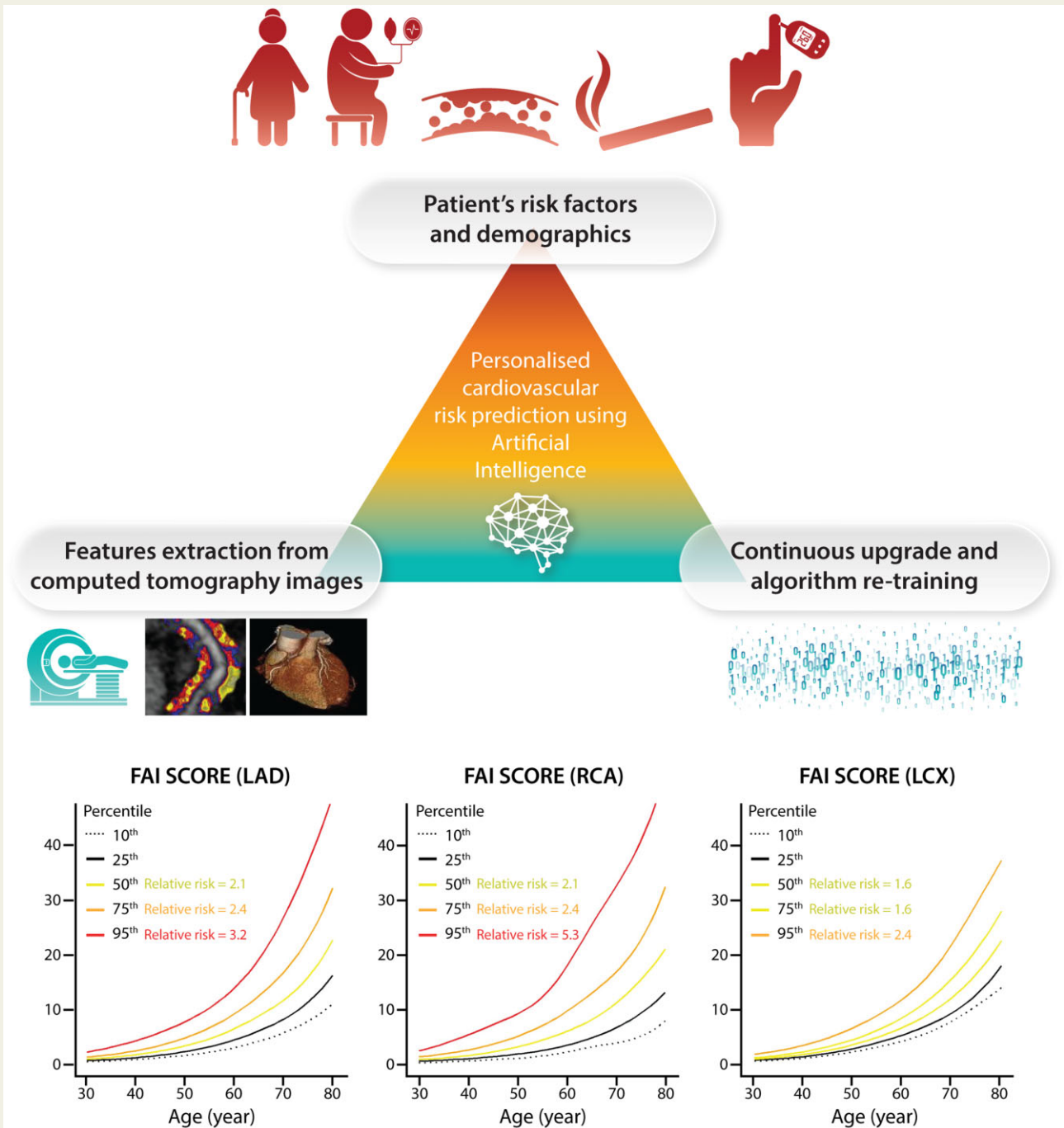
† These authors contributed equally to this work.

© The Author(s) 2021. Published by Oxford University Press on behalf of the European Society of Cardiology.

This is an Open Access article distributed under the terms of the Creative Commons Attribution License (<http://creativecommons.org/licenses/by/4.0/>), which permits unrestricted reuse, distribution, and reproduction in any medium, provided the original work is properly cited.

each coronary artery. The CaRi-Heart<sup>®</sup> device provides a reliable prediction of the patient's absolute risk for a fatal cardiac event by incorporating traditional cardiovascular risk factors along with comprehensive CCTA coronary plaque and perivascular adipose tissue phenotyping. This integration advances the prognostic utility of CCTA for individual patients and paves the way for its use as a dual diagnostic and prognostic tool among patients referred for CCTA.

**Graphical Abstract**



**Keywords**

Fat attenuation index • Pericorony • Perivascular • Atherosclerosis • Coronary artery disease

## 1. Introduction

The recognition of perivascular adipose tissue (PVAT) as an *in vivo* molecular sensor of vascular inflammation has led to the development of new imaging technologies that can detect phenotypic changes in PVAT composition, thereby allowing the non-invasive quantification of coronary inflammation.<sup>1,2</sup> Fat attenuation index (FAI) mapping, first described in 2017, was derived from studies which demonstrated that inflammatory molecules released from the human vascular wall inhibit adipogenesis and stimulate lipolysis in the adjacent PVAT. These changes modify PVAT composition from a greater lipophilic to a greater aqueous content in a spatial relationship with the inflamed vascular wall.<sup>2</sup> Since coronary computed tomography angiography (CCTA) is now a first-line investigation in the assessment of chest pain,<sup>3–5</sup> and with the prospect of using CCTA as a screening tool in high-risk asymptomatic individuals,<sup>6–8</sup> FAI provides a method to extract functional information from an existing ‘anatomical’ test with no additional scanning time or radiation exposure for the patient.

Several clinical studies have now assessed the diagnostic and prognostic utility of FAI in a range of clinical scenarios. In the largest of these studies, which included 3912 patients undergoing clinically indicated CCTA (CRISP-CT study), FAI mapping improved the prediction of adverse cardiac events beyond traditional risk factors and CCTA metrics, such as the extent of coronary atherosclerosis, coronary calcium score (CCS), and presence of high-risk plaque features.<sup>9</sup> Further studies have shown that PVAT attenuation can identify culprit lesions in patients presenting with acute myocardial infarction,<sup>2</sup> and reliably identify areas of microcalcification and inflammation.<sup>10</sup>

However, the clinical interpretation of a given FAI value depends on a range of technical factors (e.g. tube voltage, contrast media etc.), local anatomical characteristics of the coronary artery under investigation (e.g. the coronary artery segment where it is measured), and biological factors including patient demographics (e.g. age, gender, and obesity).<sup>1</sup> This limits the clinical value of uncorrected perivascular fat attenuation measurement, and calls for the development of standardized metrics to quantify the degree of coronary inflammation based on FAI mapping, to enable effective integration into the clinical workflow.<sup>11</sup>

Traditional models of primary prevention rely on the use of clinical risk factor-based prediction tools (e.g. the ESC-SCORE),<sup>12</sup> which do not capture information about the presence, extent, or nature of coronary atherosclerosis. Although imaging-derived metrics, such as CCS can be used to further stratify cardiovascular risk,<sup>13</sup> CCS predominantly reflects the presence of calcified plaques and is often increased by statin treatment.<sup>14</sup> Newer plaque interpretation scores (e.g. the Coronary Artery Disease—Reporting and Data System)<sup>15</sup> exist but are limited to quantifying the extent of coronary atherosclerotic disease and do not capture underlying clinical and biological risk factors, such as measures of coronary inflammation. In this context, quantifying the degree of vascular inflammation through perivascular FAI mapping may introduce further confusion. A new medical device, CaRi-Heart<sup>®</sup> (Caristo Diagnostics, Oxford, UK), was developed to integrate such information on clinical risk factors, coronary plaques, and the degree of coronary inflammation in a way that enables individualized estimation of a patient’s cardiac risk. We now evaluate the performance of CaRi-Heart<sup>®</sup> in a multinational cohort of patients undergoing CCTA.

## 2. Methods

### 2.1 Study population

This study included two independent cohorts of patients as part of the CRISP-CT study,<sup>9</sup> now part of the broader Oxford Risk Factors and Non-Invasive Imaging Study. The study population consisted of 3912 patients undergoing clinically indicated CCTA for evaluation of stable coronary disease in two large academic centres in Europe and the USA. The US cohort included 2040 patients undergoing CCTA at Cleveland Clinic, Cleveland, Ohio, between 2008 and 2016 [1126 (55.2%) males, median age of 53 (range: 19–87) years]. The European cohort consisted of 1872 patients [1178 (62.9%) males, median age of 62 (range: 17–89) years] who underwent CCTA between 2005 and 2009 at the Erlangen University Hospital (Erlangen, Germany). The key characteristics, presenting symptoms, and indications for the study population are summarized in *Table 1*.

Definitions of risk factors as well as adjudicated endpoints have been described elsewhere.<sup>9</sup> Briefly, cardiac mortality was defined as any death due to proximate cardiac causes (e.g. myocardial infarction, low-output heart failure, and fatal arrhythmia). Deaths fulfilling the criteria of sudden cardiac death were also included in this group.<sup>16,17</sup>

The study was approved by the respective institutional review boards (ORFAN study: South Central—Oxford C Research Ethics Committee 15/SC/0545) and local ethics committees (Cleveland Clinic IRB 17-915 & ethics committee of the Friedrich-Alexander University Erlangen-Nürnberg) and conformed to the principles outlined in the Declaration of Helsinki.

### 2.2 CaRi-Heart<sup>®</sup> device description

CaRi-Heart<sup>®</sup> is a cloud-based CE-marked medical device (Caristo Diagnostics Ltd, Oxford UK) that provides information about vascular-related inflammation from CCTA images, and calculates measures related to the risk of cardiac mortality due to coronary-related inflammation, coronary atherosclerosis, and other clinical risk factors. CT scan data can be sent electronically to the system from hospital picture archiving and communication systems (PACS) using a gateway appliance installed in the healthcare provider’s network. Reports are electronically sent back to originating PACS or by email. Although the segmentation of epicardial adipose tissue and the perivascular space is done using a deep learning network, the device includes a quality control step by a trained analyst, who checks and edits the segmentations accordingly. Segmentation and quantification of the perivascular FAI around the right coronary artery (RCA), left anterior descending artery (LAD), and left circumflex artery (LCX) were performed according to previously described protocols.<sup>2,9</sup> Three appropriately trained analysts, members of the Oxford Academic Cardiovascular CT Core Lab (OXACCT) at the University of Oxford were involved in the analysis of the present dataset, and the between-reader variability for FAI and FAI-Score are excellent (intra-class correlation coefficient ICC: 0.980,  $P < 0.001$  for the RCA, 0.990  $P < 0.001$  for the LAD, and 0.992,  $P < 0.001$  for the LCX).

The principal outputs of the CaRi-Heart<sup>®</sup> medical device are:

- (1) The FAI for the proximal segments of each of the major coronary arteries.
- (2) The FAI-Score for each of the major coronary arteries, representing the FAI weighted for technical scan parameters (e.g. tube voltage), anatomical factors related with the fat distribution around the arteries and

**Table 1** Cohort demographics and clinical characteristics

Location	American cohort Cleveland, OH, USA	European cohort Erlangen, Germany	P-value
Eligible subjects included in the study, <i>n</i> (%)	2040 (100)	1872 (100)	–
Age in years (median [range])	53 [43–62]	62 [52–68]	<0.001
Male sex, <i>n</i> (%)	1126 (55.2)	1178 (62.9)	<0.001
Risk factors* ( <i>n</i> , valid %)			
Hypertension	949 (46.5)	1068 (62.0)	<0.001
Hypercholesterolaemia	1126 (55.2)	930 (54.7)	0.78
Diabetes mellitus	219 (10.7)	215 (12.4)	0.11
Smoking	465 (22.8)	221 (12.8)	<0.001
Reason for referral			
Assessment of coronary artery disease	1761 (86.4)	1790 (95.6)	<0.001
Symptoms prior to scan			<0.001
Chest pain	1184 (58.0)	764 (43.4)	
Dyspnoea	452 (22.2)	193 (10.8)	
Medications at baseline** ( <i>n</i> , valid %)			
Antiplatelets (aspirin/clopidogrel/ticagrelor)	987 (48.4)	606 (37.6)	<0.001
Statins	813 (39.9)	557 (34.6)	0.001
ACEi or ARBs	599 (29.4)	696 (43.1)	<0.001
Beta-blockers	303 (14.9)	721 (44.8)	<0.001
Modified Duke prognostic CAD index, <i>n</i> (%)			
<50% stenosis	1044 (55.8)	1690 (82.8)	<0.001
≥2 mild stenoses with proximal CAD in 1 artery or 1 moderate stenosis	518 (27.7)	212 (10.4)	
2 moderate stenoses or 1 severe stenosis	66 (3.5)	100 (4.9)	
3 moderate stenoses, 2 severe stenoses, or severe stenosis in the proximal LAD	152 (8.1)	9 (0.4)	
3 severe stenoses or 2 severe stenoses in the proximal LAD	18 (1.0)	14 (0.7)	
≥50% stenosis in left main coronary artery	74 (3.9)	15 (0.7)	
Prospective follow-up			
Duration in months (median [range])	53.8 [4–105]	72 [51–109]	<0.001
All-cause mortality, <i>n</i> (%)	85 (4.2)	114 (6.1)	–
Cardiac mortality, <i>n</i> (%)	48 (2.4)	26 (1.4)	

Values presented as median (25th–75th percentile) or number (percentages, %); maximum missingness in the European cohort: \*9.2%, \*\*13.9%.

ACEi, Angiotensin-converting enzyme inhibitors; ARBs, angiotensin-II-receptor blockers; CAD, coronary artery disease; CT, computed tomography.

P-values are derived from Mann–Whitney *U* test (continuous variables) and Pearson's  $\chi^2$  test (categorical variables) comparisons between the two cohorts.

basic demographics (age, sex); FAI-Score is also accompanied by vessel-specific nomograms for each coronary territory to allow individualized interpretation of the degree of local coronary inflammation.

- (3) The CaRi-Heart<sup>®</sup> Risk representing the individualized patient risk of a fatal cardiac event at 8 years. This metric incorporates the FAI-Score values into a prognostic model that includes information about atherosclerotic plaque burden [as described through the modified Duke coronary artery disease (CAD) index]<sup>18</sup> and clinical risk factors (diabetes, smoking, hyperlipidaemia, and hypertension).

## 2.3 Statistical analysis

Participant demographics are summarized as numbers (percentages) or median (range or 25th–75th percentile as specified) for categorical and continuous variables, respectively (unless specified otherwise). Between-group comparisons were performed using Pearson's  $\chi^2$  for categorical variables and Mann–Whitney's test or unpaired Student's *t*-test (as appropriate) for continuous variables. Correlations between continuous predictors were assessed using Spearman's rho coefficient. Missing data

were imputed using the multiple imputation by chained equations method (package *mice* in R) with a bootstrapped logistic regression model for categorical (binary) variables and mean imputation for continuous variables.

The prognostic value of FAI-Score of each coronary artery against fatal cardiac events was then validated by using both univariate analysis as well as Cox-regression model, after inclusion of the patient risk factors into the models. The prognostic value of FAI-Score of each coronary artery is graphically summarized by plotting the log[hazard ratio (HR)] against FAI-Score, using the median FAI-Score value as reference, and the results from the Cox-regression analysis are presented as HR [95% confidence interval (95% CI)] per unit change (or standard deviation increments) of FAI-Score.

In the second part of the study, we evaluated the performance of CaRi-Heart<sup>®</sup> Risk in the USA (training) and European (testing) study populations. For validation purposes, a range of metrics are presented, including Nagelkerke's  $R^2$ , the discrimination index *D*, the unreliability index *U*, the overall quality index *Q* ( $=D-U$ ), the *C*-index (concordance)

and Somer's  $D_{xy}$  [ $=2 \times (C-0.5)$ ], and the calibration slope, all with optimism-adjustment and 95% CI calculated using bootstrapping with 200 replications. Finally, CaRi-Heart<sup>®</sup> Risk was compared to a baseline cardiac risk prediction tool consisting of age, sex, hypertension, hypercholesterolaemia, diabetes mellitus, and smoking (both with or without inclusion of CAD presence and extent)<sup>18</sup> to better understand the incremental prognostic value of comprehensive CCTA-phenotyping in this patient population. Improvement in discrimination was assessed by comparing the time-dependent C-statistic of the two models across different follow-up times, as well as by calculating the net reclassification improvement (NRI), integrated discrimination improvement (IDI), and median improvement at 8 years (95% CI calculated using bootstrapping with 200 replications).<sup>16</sup>

Finally, the net benefit of using CaRi-Heart<sup>®</sup> Risk over a baseline clinical risk model was assessed using a decision curve analysis.<sup>19</sup> In this analysis, the y axis reflects the net benefit, while the x axis reflects varying probability thresholds (for the outcome of interest, i.e. cardiac mortality

over 8 years of follow-up). The probability threshold describes the minimum probability of disease at which further intervention would be warranted. This threshold tends to be lower for interventions with high efficacy and low cost, though higher for minimally effective treatments or those associated with significant morbidity. Conversely, the net benefit reflects the difference between the expected benefit (number of patients truly at risk who will receive an intervention using the proposed strategy) and harm [number of patients without the disease who would be treated unnecessarily (false positives)], weighted by the odds of the risk threshold. This graphical method enables the comparison of the net clinical benefit of different approaches across different levels of estimated risk.

Statistical analysis was performed in the R environment (R 4.0.2, The R Foundation for Statistical Computing, <http://www.R-project.org>) using R studio (version 4.0.2) and the following packages: *rms*, *survival*, *riskRegression*, *survIDINRI*, *timeROC*, *survivalROC*, *caret*, *Hmisc*, *Design*, *rmda*.

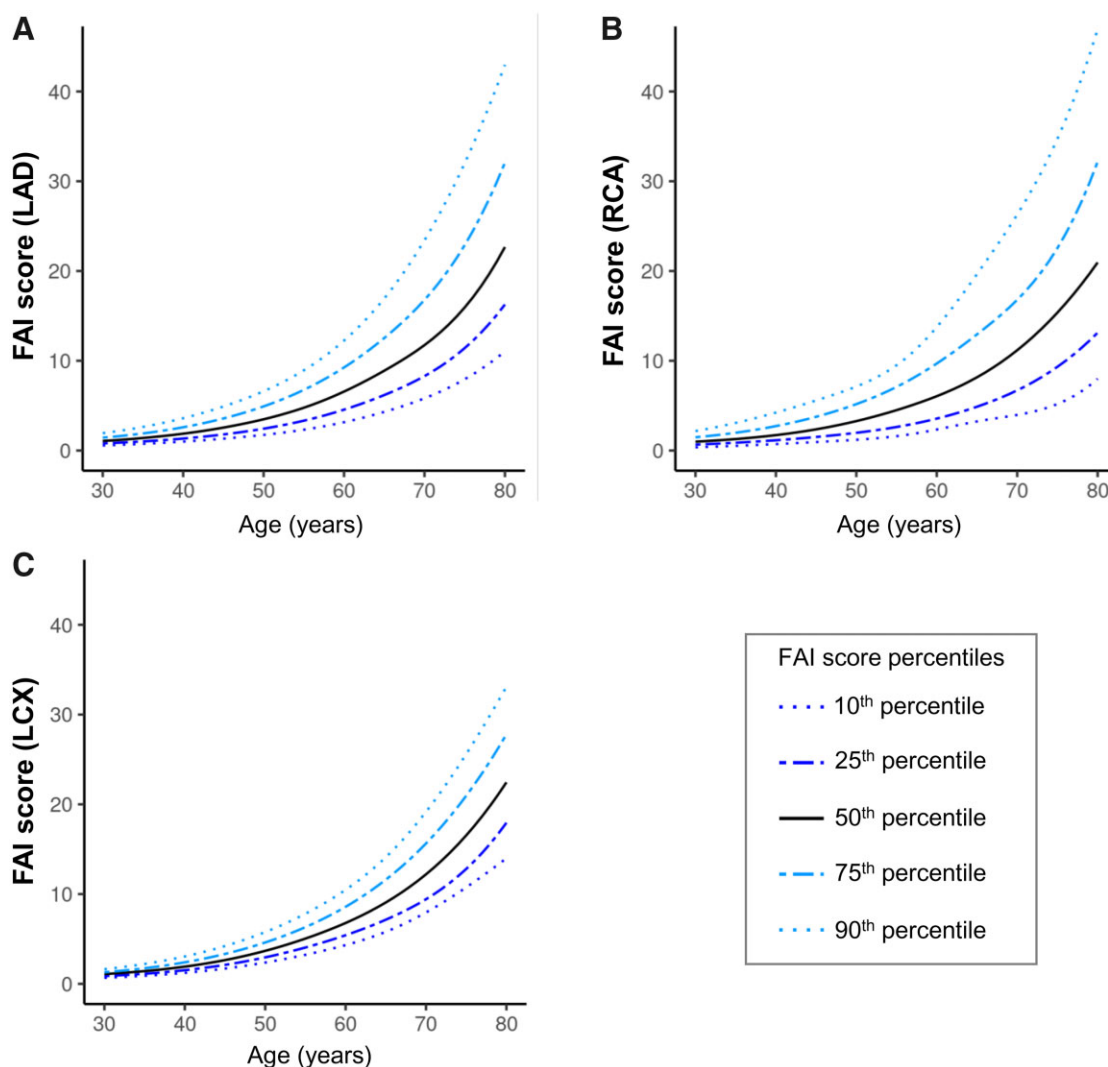


**Figure 1** FAI-Score nomograms across different age groups based on two international cohorts from Europe and the USA. Estimated nomograms with percentile curves for FAI-Score across different age strata for each one of the main coronary territories [LAD, left anterior descending artery (A); RCA, right coronary artery (B); LCX, left circumflex coronary artery (C)]. FAI, fat attenuation index.  $N = 3912$  participants per panel.

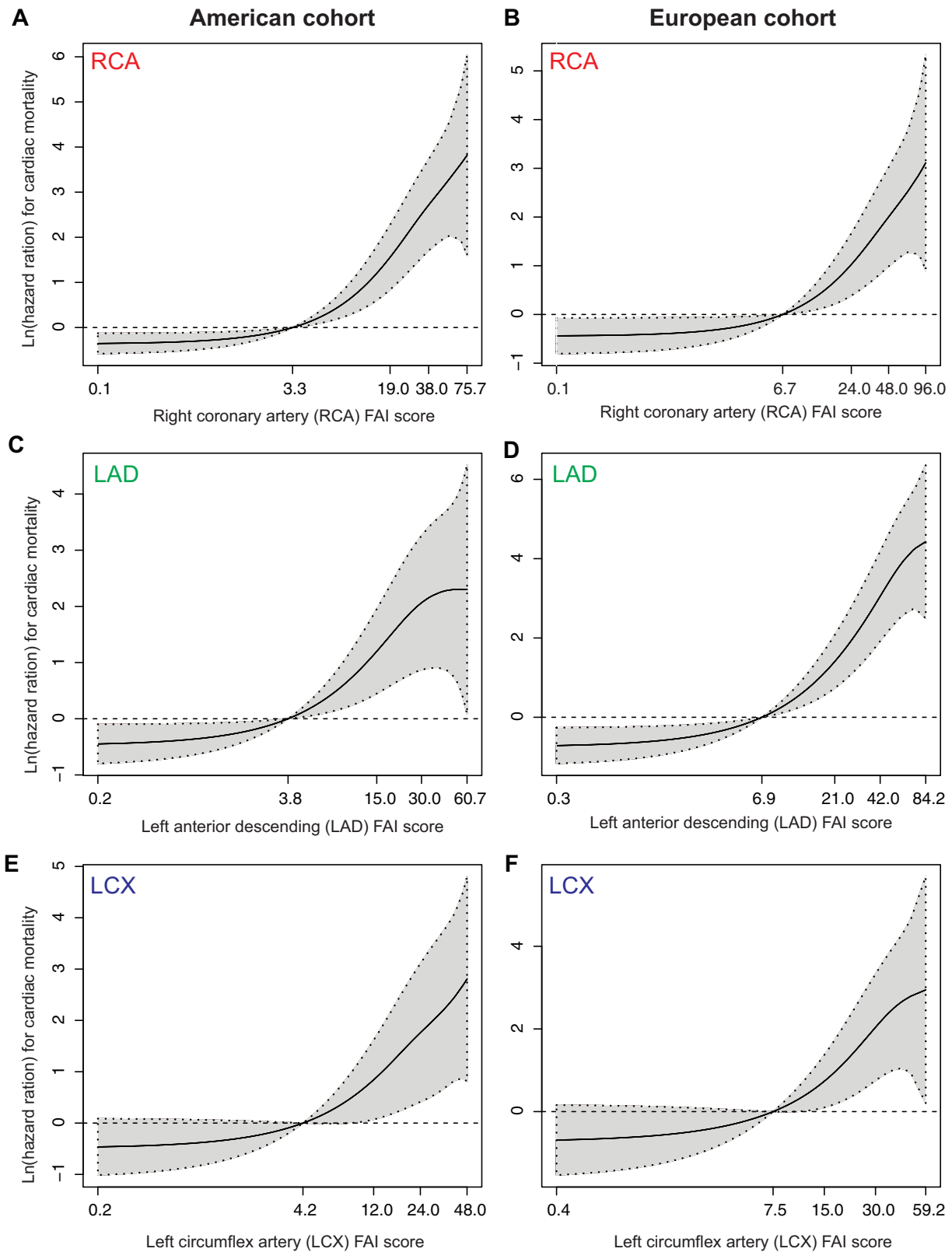


**Figure 2** Prognostic value of vessel-specific FAI-Scores for cardiac mortality. Association between FAI-Score calculated around the RCA (A and B), LAD (C and D) and LCX (E and F) in the American (A, C, and E,  $n = 2040$  participants) and European cohorts (B, D, and F,  $n = 1872$  participants). FAI: fat attenuation index.

### 3. Results

Within the US cohort of 2040 patients with a median follow-up of 53.8 months (range: 4–105 months), a total of 85 deaths were reported, 48 of which were cardiac. In the European cohort of 1872 patients with a median follow-up period of 72 months (range: 51–109 months), a total of 26 deaths were attributed to confirmed cardiac causes and 16 were

deaths of unknown cause out of a total of 114 deaths. Patient demographics are presented in *Table 1*.

#### 3.1 Standardizing FAI through the FAI-Score

To better understand how to interpret FAI-Score at an individual patient level, we calculated nomograms and percentile curves for FAI-Score around each one of the coronary vessels in a pooled analysis (*Figure 1*). As shown, FAI-Score increases with age. The associated percentile curves represent estimates of the distribution of FAI-Score in a representative sample of patients undergoing clinically indicated CCTA. Of note, FAI-Scores around the RCA, LAD, and LCX retain their prognostic value in both independent datasets, with higher scores linked to a higher subsequent risk of fatal cardiac events (*Figure 2*). This was preserved when FAI-Score for each coronary artery was used as a continuous variable in both univariate and multivariable Cox-regression (*Table 2* and *Supplementary material online, Table S1*), whereas a graded (dose-response) relationship was noted between a patient’s age- and sex-standardized FAI-Score percentile and the relative risk of cardiac mortality (*Supplementary material online, Table S2*). Notably, there was no

**Table 2 HR (and 95% CI) for risk of fatal cardiac events in the USA and European cohorts**

	US cohort (n = 2040)	European cohort (n = 1872)
FAI-score RCA	1.17 (1.13–1.21), P < 0.001	1.06 (1.04–1.08), P < 0.001
FAI-score LAD	1.11 (1.07–1.15), P < 0.001	1.07 (1.05–1.09), P < 0.001
FAI-score LCx	1.19 (1.14–1.25), P < 0.001	1.08 (1.04–1.12), P < 0.001
CaRi-Heart® risk	1.10 (1.07–1.12), P < 0.001	1.06 (1.04–1.08), P < 0.001

HR calculated per 1 unit increment in FAI-score or CaRi-Heart® risk. Unadjusted hazard ratios are reported.  
95% CI, 95% confidence interval; FAI, fat attenuation index; LAD, left anterior descending; LCx, left circumflex.

#### A Validation and calibration of the CaRi model

	Original	Training	Testing	Optimism-corrected (95% CI)
Somer’s Dxy	0.667	0.685	0.636	0.617 (0.610-0.628)
R2	0.146	0.164	0.130	0.112 (0.107-0.116)
Slope	1.000	1.000	0.873	0.873 (0.861-0.890)
Discrimination index D	0.126	0.142	0.112	0.095 (0.091-0.099)
Unreliability index U	-0.003	-0.003	0.006	0.006 (0.004-0.006)
Overall quality index Q (D-U)	0.129	0.145	0.105	0.089 (0.086-0.095)
G-index	1.457	1.642	1.393	1.208 (1.203-1.264)
AUC	0.833	0.843	0.818	0.809 (0.805-0.814)

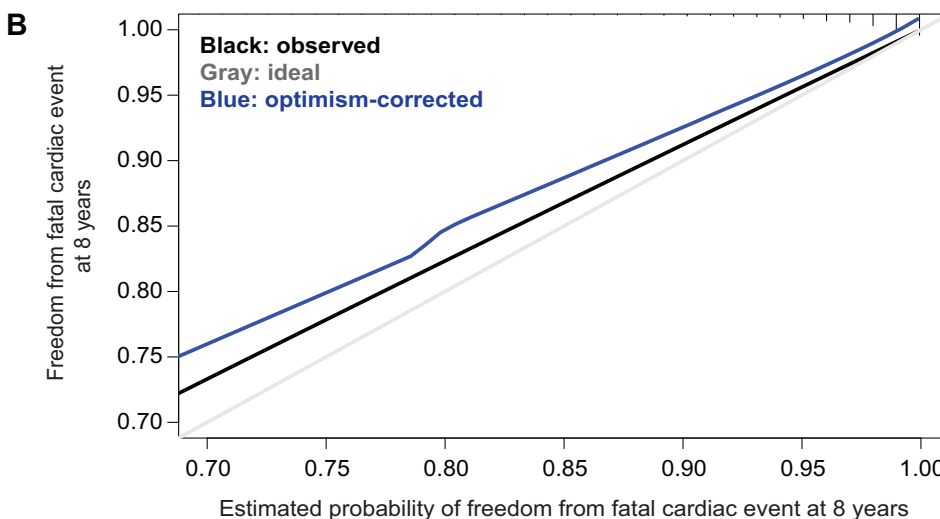


**Figure 3** Validation of the CaRi-Heart® risk. (A) Internal validation metrics in the American cohort of the CaRi-Heart® Risk describing the model’s discrimination and calibration. (B) Calibration curve of the CaRi-Heart® Risk reflecting the model-based estimated probability of cardiac mortality at 8 years vs. the actual (observed) probability across different levels of risk in our population (n = 2040). AUC, area under the curve; 95% CI, 95% confidence interval.

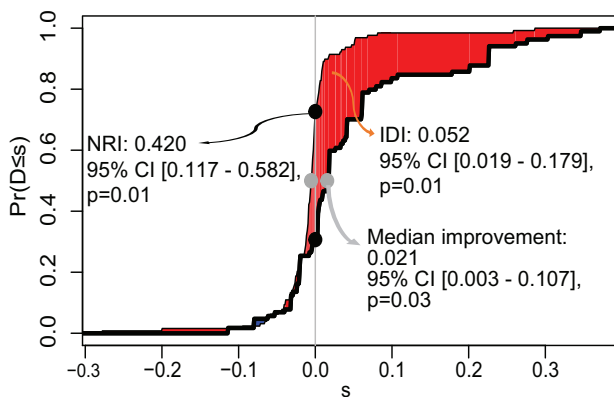
association between CCS and FAI-Score around any coronary artery (Supplementary material online, Figure S1).

### 3.2 Evaluating the prognostic value of the CaRi-Heart<sup>®</sup> device

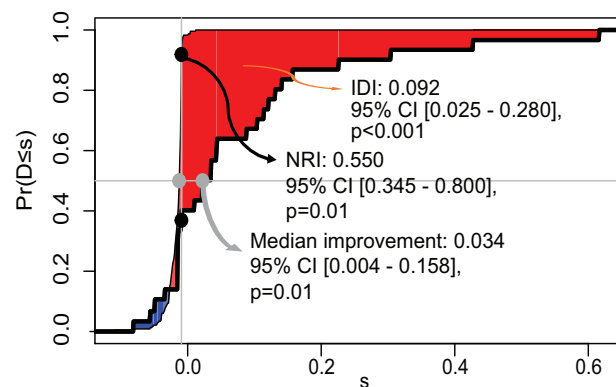
Although FAI-Score was developed as a standardized metric of coronary inflammation in each coronary artery (allowing between-subject comparisons), its prognostic value should be evaluated in the context of additional traditional risk factors (i.e. hypertension, hypercholesterolaemia, and diabetes mellitus smoking) and other CCTA features (i.e. presence

and extent of coronary atherosclerosis).<sup>18</sup> To derive an integrated risk score that encompasses all the above information for patients undergoing CCTA, the CaRi-Heart<sup>®</sup> Risk was developed to represent risk of the individual for a fatal cardiac event (at 8 years, to mirror the length of follow-up in the included cohorts). A model including all above variables was fitted in the US cohort, where it was validated internally using bootstrapping with  $n = 100$  repetitions and found to have excellent discrimination [C-statistic 0.809 (95% CI 0.805–0.814)] (Figure 3A) for prediction of cardiac mortality at 8 years. Subgroup analysis across different race and ethnicity groups is provided in Supplementary material online, Table S3. The negative predictive value of a CaRi-Heart<sup>®</sup> Risk >10% for a

**A American cohort**



**B European cohort**



**C Reclassification table**

Cohort analysed	Clinical risk model	CaRi-based model				Total	Reclassified upwards	Reclassified downwards
		<1%	1-4.99%	5-10%	>10%			
American cohort	<1%	280 (0)	110 (2)	0 (0)	0 (0)	390 (100%)	110 (28.2%)	-
	1-4.99%	159 (1)	681 (7)	107 (1)	17 (1)	964 (100%)	124 (12.9%)	159 (16.5%)
	5-10%	0 (0)	167 (1)	138 (0)	96 (7)	401 (100%)	96 (23.9%)	167 (41.6%)
	>10%	0 (0)	18 (0)	57 (3)	210 (24)	285 (100%)	-	75 (26.3%)
	Total	439 (100%)	976 (100%)	302 (100%)	323 (100%)	2040 (100%)	330 (16.2%)	401 (19.7%)
European cohort	<1%	931 (0)	126 (3)	10 (1)	1 (1)	1068 (100%)	137 (12.8%)	-
	1-4.99%	199 (2)	339 (2)	71 (3)	35 (2)	644 (100%)	106 (16.5%)	199 (30.9%)
	5-10%	6 (1)	38 (0)	28 (1)	38 (4)	110 (100%)	38 (34.6%)	44 (40.0%)
	>10%	0 (0)	6 (0)	12 (0)	32 (6)	50 (100%)	-	18 (36.0%)
	Total	1136 (100%)	509 (100%)	121 (100%)	106 (100%)	1872 (100%)	281 (15.0%)	261 (13.9%)

CaRi: cardiac risk score. Risk stratification tables presented as numbers (cases). Summaries presented as numbers (percentages, %).

**Figure 4** Incremental discriminatory value of CaRi-Heart<sup>®</sup> Risk above clinical risk predictors. Incremental discriminatory value of the CaRi-Heart<sup>®</sup> Risk for cardiac mortality ( $t = 8$  years) above a clinical risk prediction model consisting of age, sex, hypertension, hypercholesterolaemia, diabetes mellitus, and smoking in the USA (A,  $n = 2040$  participants) and European cohorts (B,  $n = 1872$  participants). The thick black line represents events, whereas the thin black line represents non-events. The difference between the black dots represents the continuous NRI, the difference between the grey dots represents the median improvement, whereas the shaded area reflects the IDI. (C) Reclassification table for discrete cardiac risk groups in the two study cohorts comparing CaRi-based risk stratification against a baseline clinical risk prediction model.

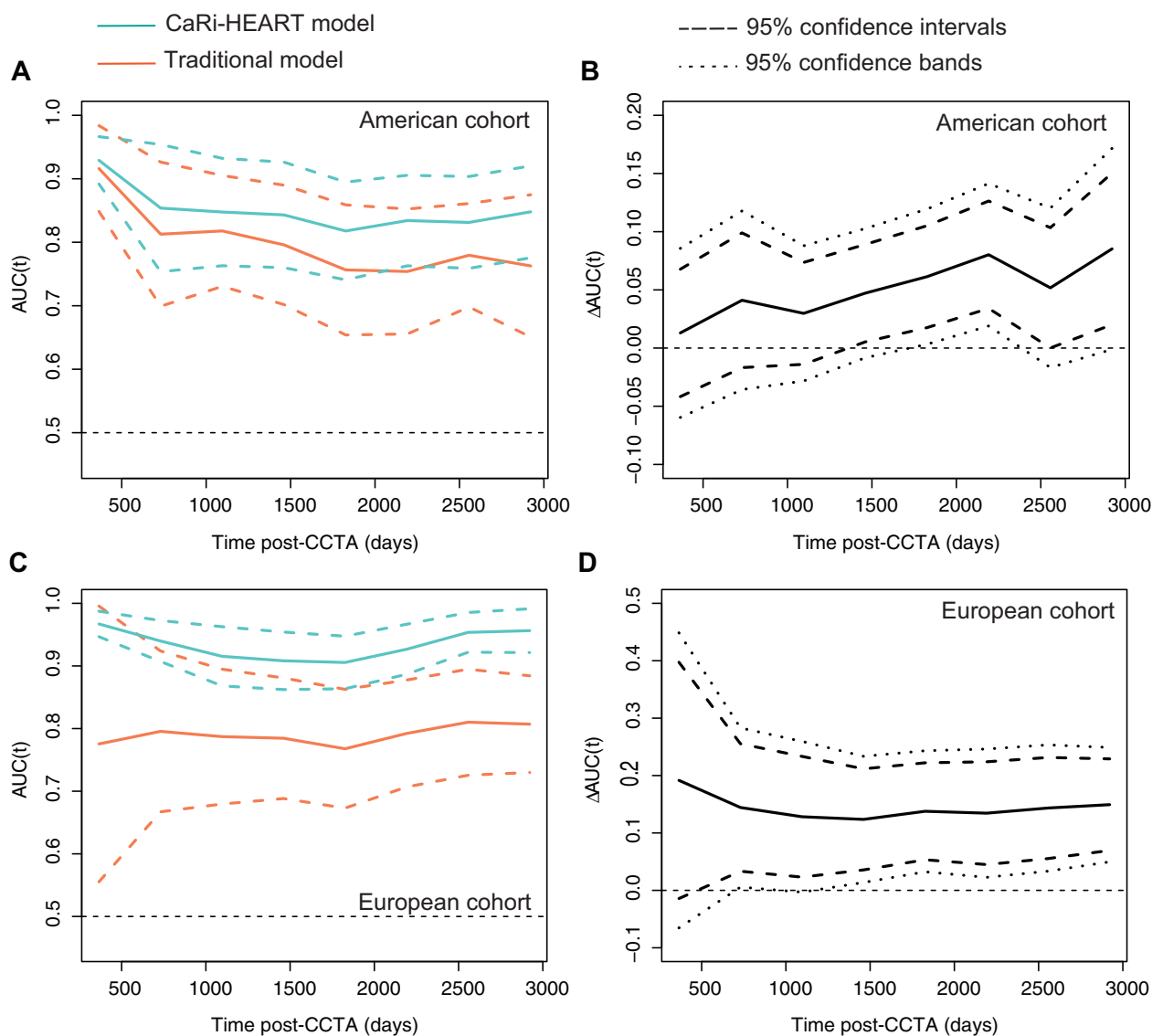


**Figure 5** Incremental discriminatory value of the CaRi-Heart<sup>®</sup> Risk across different follow-up intervals. In panel (A) the orange line reflects the calculated 'Area under the Curve (AUC)' (C-statistic) of a model consisting of baseline cardiovascular risk predictors (age, sex, hypertension, hypercholesterolaemia, diabetes mellitus, and smoking) at 1-year intervals post-CCTA in the American cohort ( $n = 2040$  participants). This is compared to the AUC for the integrated CaRi-Heart<sup>®</sup> Risk at the same follow-up times (blue line), with the difference of the AUC [ $\Delta(\text{AUC})$ ] between the two models graphically presented in panel (B). Panels (C) and (D) present the results of the same analyses in the European cohort ( $n = 1872$  participants). CCTA, coronary computed tomography angiography. Dashed lines denote 95% CI, whereas dotted lines denote confidence bands.

fatal cardiac event at 8 years was 99.3%. The CaRi-Heart<sup>®</sup>-derived risk predictions moderately overestimated risk at higher levels of predicted risk in the model calibration data (Figure 3B). When compared to a baseline risk model consisting of age, sex, hypertension, hypercholesterolaemia, diabetes mellitus, and smoking, the CaRi-Heart<sup>®</sup> Risk significantly improved risk discrimination [ $\Delta(\text{C-statistic})$  of 0.085,  $P = 0.01$  in the US Cohort and 0.149,  $P < 0.001$  in the European cohort] and classification (as assessed by the continuous NRI, IDI, and median improvement index, Figure 4) in both independent cohorts of the study. Moreover, its incremental prognostic value for prediction of cardiac mortality at 8 years persisted even after adding the modified Duke CAD index in the baseline model (Supplementary material online, Figure S2).

Across the entire study population, 611 (15.6%) patients were reclassified to a higher risk category and 662 (16.9%) were reclassified to a lower risk category by using the CaRi-Heart<sup>®</sup> Risk, compared to using a clinical risk factor-based approach (Figure 4C). The incremental value of CaRi-Heart<sup>®</sup> Risk-based approach became evident in both cohorts within 3 years of follow-up after CCTA and persisted throughout the duration of follow-up (at least until 8 years post-CCTA, Figure 5). In subgroup analysis, the CaRi-Heart<sup>®</sup> Risk retained its predictive value across all population subgroups (Figure 6). In a head-to-head comparison, CaRi-Heart<sup>®</sup> Risk significantly outperformed the predictive performance of CCS for cardiac mortality among patients that underwent both non-contrast CT and CCTA imaging (Supplementary material online, Figure S3).

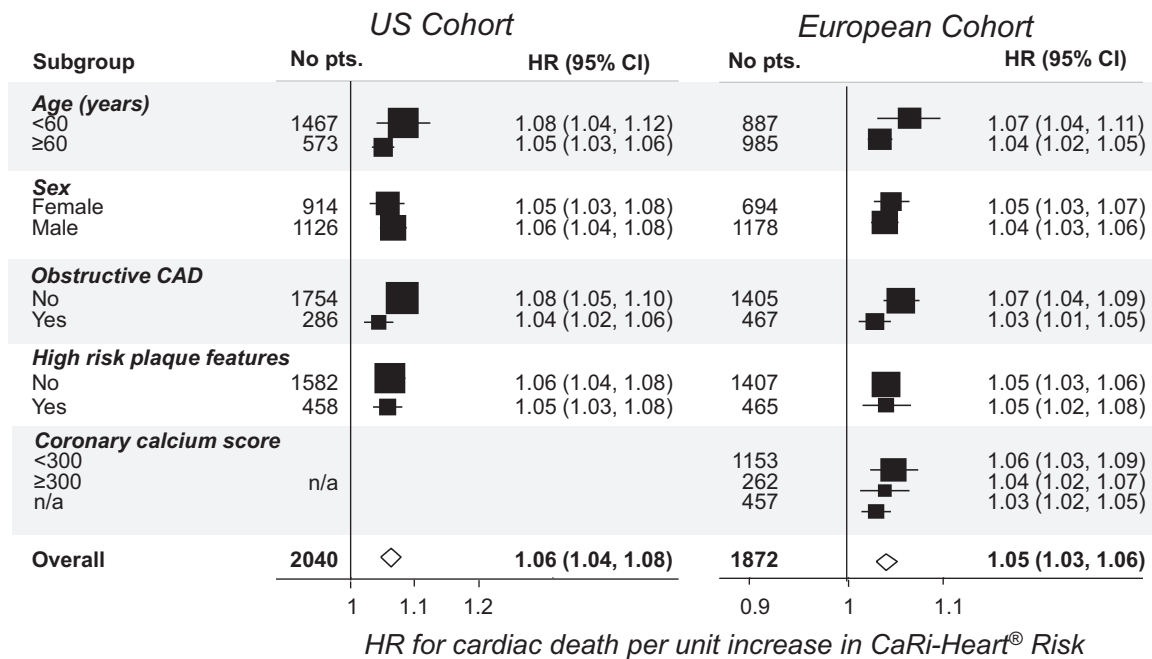


**Figure 6** Subgroup analysis for population subgroups. Predictive value of the CaRi-Heart® Risk model was retained across all population subgroups. 95% CI, 95% confidence interval; HR, hazard ratio.

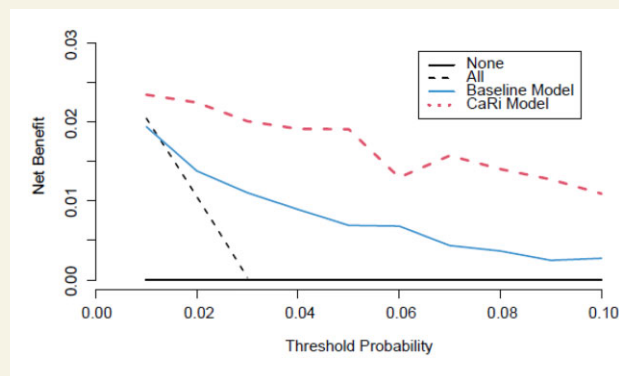


**Figure 7** Decision curve analysis of CaRi-Heart® Risk compared to a clinical prediction model. Use of the integrated CaRi-Heart® Risk is associated with consistently higher net benefit compared to a baseline risk model consisting of traditional cardiovascular risk factors (age, sex, hypertension, hypercholesterolaemia, diabetes mellitus, and smoking) across a wide range (1–10%) of cardiac mortality risk probabilities (at  $t=8$  years). Provided as a reference, the dotted line reflects the net benefit of ‘treating’ all individuals, whereas the continuous black line reflects the net benefit of treating no patients (equal to zero).

### 3.3 Net clinical benefit of the CaRi-Heart® risk

Given the limitation of traditional statistical metrics, such as calibration and discrimination, in assessing clinical value and decision analytic approaches, we performed a decision curve analysis of two alternative methods of risk stratifying individuals at risk of CAD. The first approach relied on risk

stratification of the entire study population based on traditional risk factors forming the core of most cardiovascular risk stratification tools, including age, sex, hypertension, hypercholesterolaemia, diabetes mellitus, and smoking. The second CCTA-based approach utilized CaRi-Heart® device-driven stratification. As shown in Figure 7, CaRi-Heart®-based risk stratification consistently exhibited a higher net clinical benefit across a range of threshold probabilities, therefore maximizing the identification of true positives and negatives in our population to assist with improved targeting of any preventive strategies that may be indicated.

## 4. Discussion

We validate the performance of a new medical device, CaRi-Heart®, that calculates a standardized metric of each coronary artery (FAI-Score, corrected for technical and anatomical factors as well as age and gender) and integrates these readings into a prognostic model for prediction of future fatal cardiac events, considering a patient’s atherosclerotic plaque burden and as well as clinical cardiovascular risk profile. FAI-Score for each coronary artery has significant prognostic value for 8-year cardiac mortality, providing a more standardized metric of coronary inflammation than FAI as previously described.<sup>2,20</sup> The use of this metric of coronary inflammation, in combination with a patient’s atherosclerotic plaque burden and clinical cardiovascular risk profile may provide a superior method to define a personalized risk for fatal cardiac events compared to clinical risk factors-based models, contributing to improved patient risk reclassification.

In the presence of arterial inflammation, cytokines and other mediators produced in the vascular wall by infiltrating inflammatory and other residing cells are released locally and block adipocyte differentiation in the adjacent PVAT, while stimulating lipolysis and impairing adipogenesis. This results in a

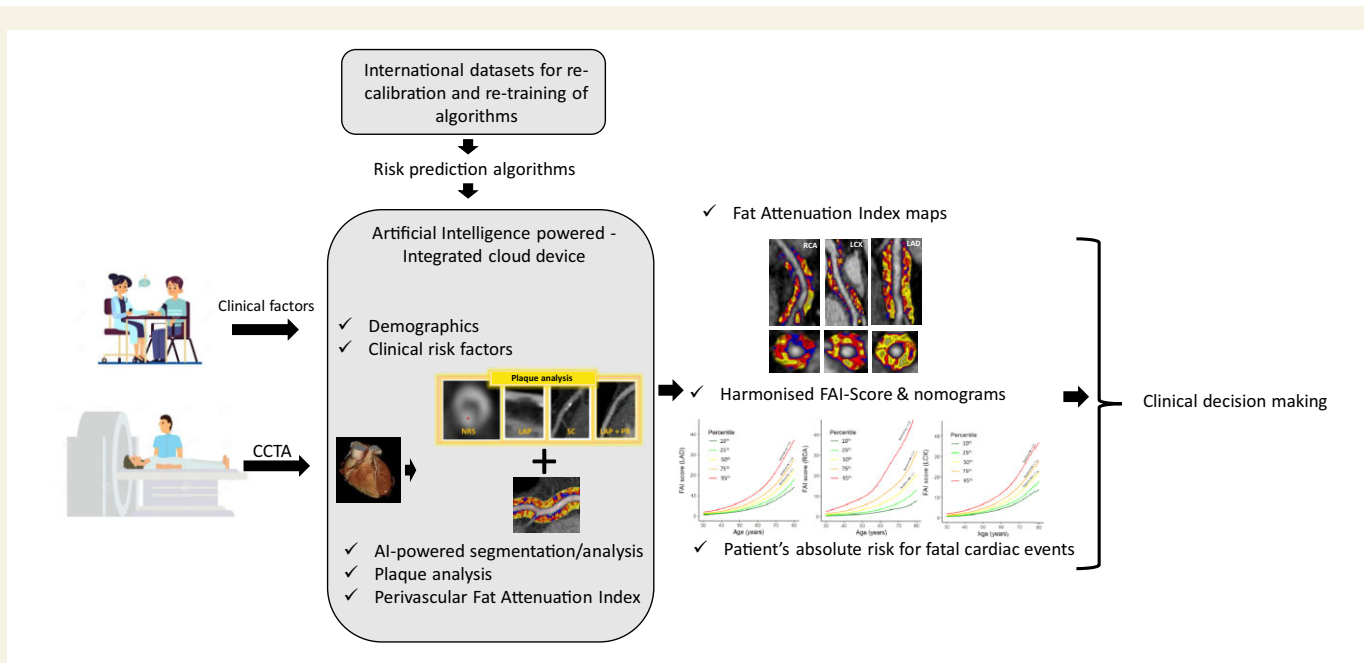


**Figure 8** The CaRi-Heart<sup>®</sup> platform. CaRi-Heart<sup>®</sup> is an automated cloud-based medical device that has been trained through deep learning to automate the segmentation of heart structures, identify the PVAT, calculate the FAI and integrate its value with scan technical details and patient demographics to provide metrics of atherosclerotic/inflammatory effects around each coronary vessel (FAI-Score), as well as an integrated cardiac risk stratification tool (CaRi-Heart<sup>®</sup> Risk).

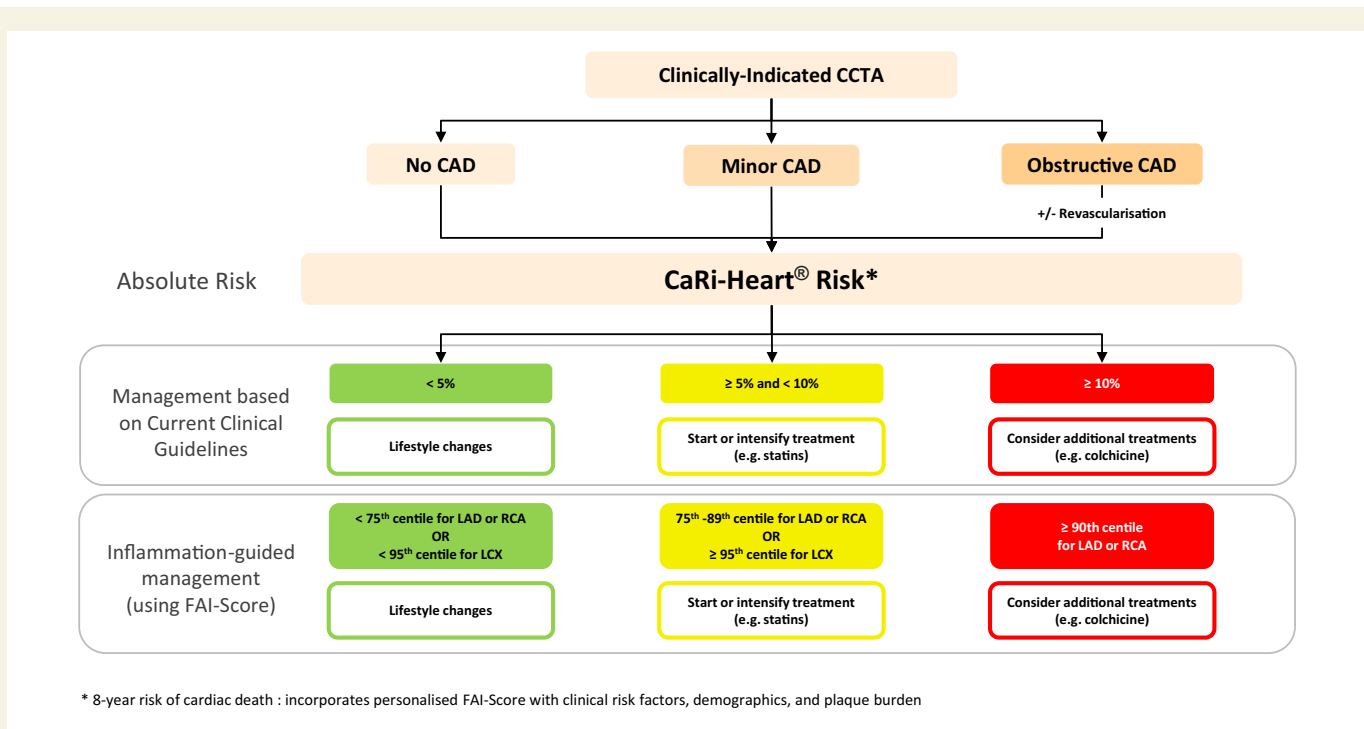


**Figure 9** Vision for incorporating FAI-Score into current clinical workflows. Among patients undergoing clinically indicated CCTA CaRi-Heart<sup>®</sup> Risk provides the individualized absolute risk for cardiac mortality based on the patient's clinical profile (i.e. demographics and traditional risk factors), CCTA plaque burden metrics and FAI-Score. The information on absolute risk for cardiac mortality can guide lifestyle and/or pharmacological changes as per clinical guidelines. FAI-Score provides an additional piece of information which reflects the levels of vascular inflammation, which is considered a new cardiovascular risk factor, accounting for the residual (inflammatory) cardiovascular risk. For instance, a young individual with no traditional risk factors may be at low absolute risk for a fatal cardiac event; however, a high FAI-Score may indicate increased relative risk for cardiac events in the long-term as a result of subclinical vascular inflammation. Hence, age- and sex-adjusted cut-offs in FAI-Score centiles may be used to guide interventions to lower vascular inflammation.

phenotypic shift in the adipose tissue composition, from a greater to a lesser lipophilic content and therefore a higher aqueous/lipid ratio. On CT imaging, this shift can be detected as spatial changes in PVAT attenuation from lower (closer to -190 HU) to higher (closer to -30 HU) attenuation values. Pericoronary FAI mapping applies this concept around standardized coronary segments on CCTA, where it calculates weighted attenuation changes linked to the inflammatory status of the adjacent vessel wall.<sup>2</sup>

Following its initial description, several clinical studies have explored the diagnostic and prognostic implications of FAI mapping. The first and largest of these studies (CRISP-CT study) showed that higher pericoronary FAI values (reflective of a higher inflammatory/atherosclerotic burden) were associated with a higher incidence of cardiac-specific adverse outcomes as well as all-cause mortality among patients undergoing CCTA in two large centres in Europe and the USA.<sup>9</sup> Statistical analyses revealed that the residual risk detected through FAI mapping was not adequately explained by age, sex, traditional risk factors, coronary calcium, high-risk plaque features, or the extent of coronary atherosclerosis on CCTA. This highlighted how FAI provided an effective way to extract meaningful prognostic information from a common non-invasive imaging modality already performed as part of routine clinical care, at no increased cost or radiation exposure. Subsequent studies have shown that pericoronary fat attenuation is closely linked to coronary inflammation and microcalcification as measured by <sup>18</sup>F-NaF uptake on PET-CT,<sup>10</sup> predicts the progression of coronary atherosclerosis,<sup>21</sup> can track the presence of culprit lesions among patients presenting with acute myocardial infarction,<sup>22,23</sup> stratifies the cardiac risk associated with a high-risk plaque phenotype,<sup>24</sup> and is modifiable through targeted anti-inflammatory treatments.<sup>25,26</sup>

As the use and application of pericoronary fat mapping continues to expand, there is an urgent need to standardize its reporting, while acknowledging potentially important confounders. While the process of perivascular fat attenuation analysis can be easily done by different operators and platforms (with consistent prognostic value across different age, sex, and race groups)<sup>9,27,28</sup> the interpretation of a given PVAT attenuation value ultimately relies on the patient's age, sex, cardiometabolic status, and technical variables related with the actual scan acquisition.<sup>1,29</sup> While the CRISP-CT study proposed a cut-off of -70.1 HU as a critical threshold to identify high-risk individuals,<sup>9</sup> generalization of this cut-off may be limited by the fact that this has not been adjusted for the above-mentioned factors in other independent studies.

A new medical device, CaRi-Heart<sup>®</sup>, now calculates the adjusted FAI-Score for each coronary artery, projected in nomograms according to age. Indeed, the percentile curves provided in this study may be used in independent studies to harmonize the reporting of pericoronary FAI mapping across different patient and investigator groups. We now validate FAI-Score, and we demonstrate a strong prognostic value for cardiac mortality. Unlike FAI (which was previously shown to lose its prognostic value when measured around the LCX),<sup>9</sup> FAI-Score around each one of the major coronary arteries is consistently associated with future cardiac mortality risk. However, clinical interpretation of FAI-Score can only be undertaken in a standardized way, and we now provide nomograms to allow interpretation of the results across patients of different ages.

Furthermore, integrating the above information into a prognostic model that also accounts for a patient's demographics, risk factors, and atherosclerotic plaque burden, would provide a meaningful clinical tool to guide deployment of primary or secondary prevention treatments. CaRi-Heart<sup>®</sup> provides the CaRi-Heart<sup>®</sup> Risk, which is the patient's 8-years individualized risk for a fatal cardiac event. The algorithm was originally trained in the American cohort and then validated in the

European cohort. Indeed, CaRi-Heart<sup>®</sup> Risk reclassifies ~16% of the subjects undergoing CCTA to a higher risk category, and ~17% to lower risk category compared to a clinical risk factor-based model, when applied in the European cohort i.e. nearly a third of the total population. Our analysis also shows that, for both low and high-risk individuals, CaRi-Heart-guided risk stratification consistently provides a higher level of net clinical benefit (compared to standard clinical risk models) across a range of thresholds probabilities for clinical decision making (Figure 8).

Further to the calculation of the individualized absolute risk for cardiac mortality as a means to guide deployment of appropriate cardiovascular risk reduction strategies, FAI-Score provides a standalone, standardized metric of coronary inflammation. This information may be particularly useful in select patient groups, such as young individuals with evidence of inflammation but no other traditional risk factors, who despite being at low absolute risk are nonetheless at high relative risk compared to individuals of similar age and sex. In such patients, the decision to initiate therapy may be driven by the presence of a strong biological risk factor, such as elevated LDL cholesterol levels in young patients with familial hypercholesterolaemia, independent of the absolute risk score calculated through standard tools (Figure 9). Newer prospectively designed cohorts within the ORFAN study are also underway to further examine the value of CaRi-Heart<sup>®</sup> in more ethnically diverse cohorts and when added to quantitative circulating biomarkers.

## 5. Conclusion

CaRi-Heart<sup>®</sup>, a novel CCTA-based risk stratification medical device, integrates the recently described FAI mapping with traditional cardiovascular risk factors and multi-dimensional, comprehensive CCTA coronary plaque analysis. The prognostic output produced by CaRi-Heart<sup>®</sup> demonstrates significant net clinical benefit in two large and independent CCTA populations over and above traditional cardiovascular risk factors. Integration of CaRi-Heart<sup>®</sup> analyses into current clinical pathways has the potential to advance the prognostic utility of CCTA analysis in the investigation and management of CAD risk.

## Supplementary material

Supplementary material is available at Cardiovascular Research online.

## Authors' contributions

E.K.O and A.S.A. contributed to the study design, image/data analysis, statistical analysis, and writing of the manuscript; D.S. contributed to the statistical analysis. L.V.K. contributed to image analysis. C.S., S.N., K.M.C., M.Y.D., S.A., and J.D. provided scientific direction and contributed to writing the manuscript; M.M., S.A., and M.Y.D. co-ordinated the collection of clinical data and CT scans; M.S., P.T., and C.M. coordinated the technical development of the CaRi-Heart Medical Device; C.A. designed the study, raised the funding for image and data analysis, coordinated and directed the project, supervised the image analysis and wrote the manuscript.

**Conflict of interest:** The methods for analysis of the perivascular FAI described in this report are subject to patent PCT/GB2015/052359 and patent applications PCT/GB2017/053262, GB2018/1818049.7, GR20180100490, and GR20180100510, licenced through exclusive licence to Caristo Diagnostics. C.A., K.M.C., C.S. and S.N. are founders, shareholders, and directors of Caristo Diagnostics, a CT image analysis

company. J.D. and E.K.O. are shareholders and consultants at Caristo Diagnostics. A.S.A declares consultancy with Caristo Diagnostics. J.D. and M.Y.D. are members of the advisory board of Caristo Diagnostics. C.S., P.T., M.S., C.M., and D.S. are employees of Caristo Diagnostics. The remaining authors have nothing to disclose.

## Funding

This work was supported by the British Heart Foundation (FS/16/15/32047, TG/16/3/32687, TG/19/2/34831 and RG/F/21/110040 to CA), the National Institute for Health Research Oxford Biomedical Research Centre (Oxford, United Kingdom) and Innovate UK. M.Y.D. is supported by the Haslam Family endowed chair in cardiovascular medicine. Portions of this research were funded by a generous philanthropic gift by the Holekamp family. The study was supported by Caristo Diagnostics, who has provided the CaRi-Heart<sup>®</sup> analyses.

## Data availability

Supporting data for this manuscript will be made available by the corresponding author upon reasonable request.

## References

- Antoniades C, Antonopoulos AS, Deanfield J. Imaging residual inflammatory cardiovascular risk. *Eur Heart J* 2020;**41**:748–758.
- Antonopoulos AS, Sanna F, Sabharwal N, Thomas S, Oikonomou EK, Herdman L, Margaritis M, Shirodaria C, Kampoli AM, Akoumianakis I, Petrou M, Sayeed R, Krasopoulos G, Psarros C, Ciccone P, Brophy CM, Digby J, Kelion A, Uberoi R, Anthony S, Alexopoulos N, Tousoulis D, Achenbach S, Neubauer S, Channon KM, Antoniades C. Detecting human coronary inflammation by imaging perivascular fat. *Sci Transl Med* 2017;**9**:eaal2658.
- National Institute for Health and Care Excellence (NICE). Chest Pain of Recent Onset: Assessment and diagnosis. *Clinical guideline [CG95]*, 2016.
- Moss AJ, Williams MC, Newby DE, Nicol ED. The updated NICE guidelines: cardiac CT as the first-line test for coronary artery disease. *Curr Cardiovasc Imaging Rep* 2017;**10**:15.
- Knuuti J, Wijns W, Saraste A, Capodanno D, Barbato E, Funck-Brentano C, Prescott E, Storey RF, Deaton C, Cuisset T, Agewall S, Dickstein K, Edvardsen T, Escaned J, Gersh BJ, Svitil P, Gilard M, Hasdai D, Hatala R, Mahfoud F, Masip J, Muneretto C, Valgimigli M, Achenbach S, Bax JJ, Group ESCSD. 2019 ESC Guidelines for the diagnosis and management of chronic coronary syndromes. *Eur Heart J* 2019;**41**:407–477.
- Bergstrom G, Berglund G, Blomberg A, Brandberg J, Engstrom G, Engvall J, Eriksson M, de Faire U, Flinck A, Hansson MG, Hedblad B, Hjelmgren O, Janson C, Jernberg T, Johnsson A, Johansson L, Lind L, Lofdahl CG, Melander O, Ostgren CJ, Persson A, Persson M, Sandstrom A, Schmidt C, Soderberg S, Sundstrom J, Toren K, Waldenstrom A, Wedel H, Vikgren J, Fagerberg J, Fagerberg B, Rosengren A. The Swedish CardioPulmonary BioImage Study: objectives and design. *J Intern Med* 2015;**278**:645–659.
- Scot-Heart investigators. CT coronary angiography in patients with suspected angina due to coronary heart disease (SCOT-HEART): an open-label, parallel-group, multicentre trial. *Lancet* 2015;**385**:2383–2391.
- Newby DE, Adamson PD, Berry C, Boon NA, Dweck MR, Flather M, Forbes J, Hunter A, Lewis S, MacLean S, Mills NL, Norrie J, Roditi G, Shah ASV, Timmis AD, van Beek EJ, Williams MC, Scot-Heart Investigators. Coronary CT angiography and 5-year risk of myocardial infarction. *N Engl J Med* 2018;**379**:924–933.
- Oikonomou EK, Marwan M, Desai MY, Mancio J, Alashi A, Hutt Centeno E, Thomas S, Herdman L, Kotanidis CP, Thomas KE, Griffin BP, Flamm SD, Antonopoulos AS, Shirodaria C, Sabharwal N, Deanfield J, Neubauer S, Hopewell JC, Channon KM, Achenbach S, Antoniades C. Non-invasive detection of coronary inflammation using computed tomography and prediction of residual cardiovascular risk (the CRISP CT study): a post-hoc analysis of prospective outcome data. *Lancet* 2018;**392**:929–939.
- Kwiccinski J, Dey D, Cadet S, Lee SE, Otaki Y, Huynh PT, Doris MK, Eisenberg E, Yun M, Jansen MA, Williams MC, Tamarappoo BK, Friedman JD, Dweck MR, Newby DE, Chang HJ, Slomka PJ, Berman DS. Peri-coronary adipose tissue density is associated with (18)F-sodium fluoride coronary uptake in stable patients with high-risk plaques. *JACC Cardiovasc Imaging* 2019;**12**:2000–2010.
- Antoniades C, Shirodaria C. Detecting coronary inflammation with perivascular fat attenuation imaging: making sense from perivascular attenuation maps. *JACC Cardiovasc Imaging* 2019;**12**:2011–2014.
- Conroy RM, Pyorala K, Fitzgerald AP, Sans S, Menotti A, De BG, De BD, Ducimetiere P, Jousilahti P, Keil U, Njolstad I, Oganov RG, Thomsen T, Tunstall PH, Tverdal A, Wedel H, Whincup P, Wilhelmsen L, Graham IM, SCORE project group. Estimation of ten-year risk of fatal cardiovascular disease in Europe: the SCORE project. *Eur Heart J* 2003;**24**:987–1003.
- Greenland P, LaBree L, Azen SP, Doherty TM, Detrano RC. Coronary artery calcium score combined with Framingham score for risk prediction in asymptomatic individuals. *JAMA* 2004;**291**:210–215.
- Alexopoulos N, Melek BH, Arepalli CD, Hartlage GR, Chen Z, Kim S, Stillman AE, Raggi P. Effect of intensive versus moderate lipid-lowering therapy on epicardial adipose tissue in hyperlipidemic post-menopausal women: a substudy of the BELLES trial (Beyond Endorsed Lipid Lowering with EBT Scanning). *J Am Coll Cardiol* 2013;**61**:1956–1961.
- Cury RC, Abbara S, Achenbach S, Agatston A, Berman DS, Budoff MJ, Dill KE, Jacobs JE, Maroules CD, Rubin GD, Rybicki FJ, Schoepf UJ, Shaw LJ, Stillman AE, White CS, Woodard JK, Leipsic JA. CAD-RADS(TM) Coronary Artery Disease - Reporting and Data System. An expert consensus document of the Society of Cardiovascular Computed Tomography (SCCT), the American College of Radiology (ACR) and the North American Society for Cardiovascular Imaging (NASCI). Endorsed by the American College of Cardiology. *J Cardiovasc Comput Tomogr* 2016;**10**:269–281.
- Cutlip DE, Windecker S, Mehran R, Boam A, Cohen DJ, van Es GA, Steg PG, Morel MA, Mauri L, Vranckx P, McFadden E, Lansky A, Hamon M, Krucoff MW, Serruys PW, Academic Research Consortium. Clinical end points in coronary stent trials: a case for standardized definitions. *Circulation* 2007;**115**:2344–2351.
- Hicks KA, Tchong JE, Bozkurt B, Chaitman BR, Cutlip DE, Farb A, Fonarow GC, Jacobs JP, Jaff MR, Lichtman JH, Limacher MC, Mahaffey KW, Mehran R, Nissen SE, Smith EE, Targum SL. 2014 ACC/AHA Key Data Elements and Definitions for Cardiovascular Endpoint Events in Clinical Trials: a Report of the American College of Cardiology/American Heart Association Task Force on Clinical Data Standards (Writing Committee to Develop Cardiovascular Endpoints Data Standards). *J Am Coll Cardiol* 2015;**66**:403–469.
- Min JK, Shaw LJ, Devereux RB, Okin PM, Weinsaft JW, Russo DJ, Lippolis NJ, Berman DS, Callister TQ. Prognostic value of multidetector coronary computed tomographic angiography for prediction of all-cause mortality. *J Am Coll Cardiol* 2007;**50**:1161–1170.
- Vickers AJ, Elkin EB. Decision curve analysis: a novel method for evaluating prediction models. *Med Decis Making* 2006;**26**:565–574.
- Oikonomou EK, Antoniades C. The role of adipose tissue in cardiovascular health and disease. *Nat Rev Cardiol* 2019;**16**:83–99.
- Goeller M, Tamarappoo BK, Kwan AC, Cadet S, Commandeur F, Razipour A, Slomka PJ, Gransar H, Chen X, Otaki Y, Friedman JD, Cao JJ, Albrecht MH, Bittner DO, Marwan M, Achenbach S, Berman DS, Dey D. Relationship between changes in pericoronary adipose tissue attenuation and coronary plaque burden quantified from coronary computed tomography angiography. *Eur Heart J Cardiovasc Imaging* 2019;**20**:636–643.
- Goeller M, Achenbach S, Cadet S, Kwan AC, Commandeur F, Slomka PJ, Gransar H, Albrecht MH, Tamarappoo BK, Berman DS, Marwan M, Dey D. Pericoronary adipose tissue computed tomography attenuation and high-risk plaque characteristics in acute coronary syndrome compared with stable coronary artery disease. *JAMA Cardiol* 2018;**3**:858–863.
- Oikonomou EK, Williams MC, Kotanidis CP, Desai MY, Marwan M, Antonopoulos AS, Thomas KE, Thomas S, Akoumianakis I, Fan LM, Kesavan S, Herdman L, Alashi A, Centeno EH, Lyasheva M, Griffin BP, Flamm SD, Shirodaria C, Sabharwal N, Kelion A, Dweck MR, Van Beek EJ, Deanfield J, Hopewell JC, Neubauer S, Channon KM, Achenbach S, Newby DE, Antoniades C. A novel machine learning-derived radiotranscriptomic signature of perivascular fat improves cardiac risk prediction using coronary CT angiography. *Eur Heart J* 2019;**40**:3529–3543.
- Oikonomou EK, Desai MY, Marwan M, Kotanidis CP, Antonopoulos AS, Schottlander D, Channon KM, Neubauer S, Achenbach S, Antoniades C. Perivascular fat attenuation index stratifies cardiac risk associated with high-risk plaques in the CRISP-CT study. *J Am Coll Cardiol* 2020;**76**:755–757.
- Elnabawi YA, Oikonomou EK, Dey AK, Mancio J, Rodante JA, Aksentjevich M, Choi H, Keel A, Erb-Alvarez J, Teague HL, Joshi AA, Playford MP, Lockshin B, Choi AD, Gelfand JM, Chen MY, Bluemke DA, Shirodaria C, Antoniades C, Mehta NN. Association of biologic therapy with coronary inflammation in patients with psoriasis as assessed by perivascular fat attenuation index. *JAMA Cardiol* 2019;**4**:885–891.
- Dai X, Yu L, Lu Z, Shen C, Tao X, Zhang J. Serial change of perivascular fat attenuation index after statin treatment: insights from a coronary CT angiography follow-up study. *Int J Cardiol* 2020;**319**:144–149.
- Tzolos E, McElhinney P, Williams MC, Cadet S, Dweck MR, Berman DS, Slomka PJ, Newby DE, Dey D. Repeatability of quantitative pericoronary adipose tissue attenuation and coronary plaque burden from coronary CT angiography. *J Cardiovasc Comput Tomogr* 2021;**15**:81–84.
- Goeller M, Rahman I, Dayhid A, Cadet S, Lin A, Adams D, Thakur U, Yap G, Marwan M, Achenbach S, Dey D, Ko B. Pericoronary adipose tissue and quantitative global non-calcified plaque characteristics from CT angiography do not differ in matched South Asian, East Asian and European-origin Caucasian patients with stable chest pain. *Eur J Radiol* 2020;**125**:108874.
- Ma R, Ties D, van Assen M, Pelgrim GJ, Sidorenkov G, van Ooijen PMA, van der Harst P, van Dijk R, Vliegenthart R. Towards reference values of pericoronary adipose tissue attenuation: impact of coronary artery and tube voltage in coronary computed tomography angiography. *Eur Radiol* 2020;**30**:6838–6846.